ISSN 0965-545X, Polymer Science, Ser. A, 2012, Vol. 54, No. 9, pp. 684–692. © Pleiades Publishing, Ltd., 2012.
Original Russian Text © S.A. Khatipov, S.A. Serov, N.V. Sadovskaya, E.M. Konova, 2012, published in Vysokomolekulyarnye Soedineniya, Ser. A, 2012, Vol. 54, No. 9, pp. 1360–1369.

Morphology of Irradiated Polytetrafluoroethylene[1]

S. A. Khatipov*, S. A. Serov, N. V. Sadovskaya, and E. M. Konova

State Research Center—Karpov Institute of Physical Chemistry, per. Obukha 3, 105064 Moscow, Russia

**e-mail: khatipov@cc.nifhi.ac.ru*

Received October 6, 2011;
Revised Manuscript Received February 6, 2012

Abstract—Supramolecular structures and morphologies of nonsintered, sintered, and radiation-modified suspension-polymerized PTFEs are investigated via scanning electron microscopy. Gamma irradiation is performed below and above the melting point of the crystalline phase. The fibrillar supramolecular structure of the nonsintered PTFE is preserved after its sintering. However, some regions of fibrils in the sintered PTFE form lamellas elongated perpendicularly to the orientation of fibrils. Irradiation of PTFE below the melting temperature at 20 and 200°C is not accompanied by a qualitative change in its morphology. Irradiation above the melting temperature results in reorganization of the PTFE structure, namely, formation of spherulites consisting of radially oriented fibrils.

DOI: 10.1134/S0965545X12080044

INTRODUCTION

Recent years have seen considerable interest in the study of PTFE irradiated by heavy-ion, gamma, and electron radiation [1–4]. Such careful attention is due to the finding that some practically important properties of a polymer are considerably improved after its irradiation in the temperature range above the melting point [5–10]. The main emphasis was put on molecular mechanisms and molecular structure [4, 11–14]. At the same time, it should be noted that the macroscopic properties of a polymer depend on its supramolecular structure and morphology. Therefore, research into the morphologies of radiation-modified PTFEs, like clarification of molecular mechanisms, is of independent interest.

The morphology of the original nonirradiated PTFE has been studied for already half a century [15–19]. In [15], for the first time, the morphology of melt-crystallized PTFE was studied by electron microscopy. The existence of bands with striation structure was found. The bands were interpreted as faces of crystalline lamellas (lamellar single crystals). In contrast, the authors of [16, 17] concluded that the bands consist of fibrillar crystallites packed in parallel. In this case, the striations are related to interfibrillar amorphous regions. In [20], by analogy with PE, the authors recurred to the interpretation of bands as faces of crystalline lamellas and striations due to fracture. Later on, this viewpoint became prevalent [19, 21, 22]. However, on the basis of studies of the supramolecular structure and morphology of raw PTFE particles, it was inferred that the fibrillar structure is preserved after sintering [23].

There is a common opinion about the morphology of polymerizate particles (nonsintered raw PTFE), as opposed to that of the sintered PTFE (crystallized from melt), that PTFE possesses a fibrillar structure before sintering [18–20, 23, 24].

In the present paper, a comparative investigation of the morphologies of polymerizate particles, sintered PTFE, and its irradiated modifications obtained at different irradiation temperatures is performed.

EXPERIMENTAL

Research Objects

Suspension-polymerized high-molecular-mass PTFE particles subjected to neither milling nor heating to the melting temperature of crystallites were investigated. The powder (provided by OAO Galogen, Perm, Russia) was synthesized via a standard procedure.

Bulk samples of the sintered PTFE were produced by the Kirovo-Chepetsk Chemical Works from the powder of the PN brand through uniaxial powder molding followed by sintering.

The molecular masses of the original PTFE samples determined from the heat of crystallization [25] were

$$M_n = 2.1 \times 10^{11}(\Delta H_c)^{-5.16} = 1.2 \times 10^7.$$

[1] This work was supported by the federal target program Studies and Investigations of Development of the Science and Technology Complex of Russia for 2007–2012 (State Contract no. 02.523.12.3024 from 0.60.8.2009).

Irradiation

Sintered PTFE samples were irradiated at 20, 200, and 335°C in an inert medium (argon) on a KSV-500 γ-ray unit (Karpov Institute of Physical Chemistry) with Co-60 with γ-quanta with an average energy of 1.25 MeV. The samples were placed in a radiation-chemical apparatus [26] whose construction made it possible to set the required conditions of irradiation. The radiation dose rate was 2.8 Gy/s.

Scanning Electron Microscopy

The morphologies of PTFE samples were investigated by the method of scanning electron microscopy (SEM). Fracture surfaces were obtained in liquid nitrogen. Images of the fracture surfaces were measured on a Jeol JSM-7500F high-resolution scanning electron microscope (Japan) with a field-emission cathode. The images were obtained in the regime of low-energy secondary electrons because this regime provided the highest resolution (1.5 and 1 nm at primary-beam energies of 1 and 5 keV, respectively). In order to exclude charging effects and electron-beam damage of the objects, the following methodological approaches were employed: Measurements were performed at a low electron-beam current (3×10^{-11} A), which was provided by the presence of a cold field-emission cathode. In addition, a special gentle-beam regime, in which probe electrons were slowed down directly near the sample surface, was activated. As a result, on the one hand, the energy of primary electrons was reduced to ultralow values, thereby leading to a decrease in charging effects and exclusion of the sample damage. On the other hand, the electron-probe diameter remained low; thus, high resolution was preserved. Finally, a metallic platinum film was magnetron-deposited on the fracture surface.

During the deposition of platinum, the parameters were set as follows: an electric current of 30 μA, a deposition time of 20 s, a target-to-sample distance of 40 cm, and a pressure of 5 Pa. A platinum film ~5 nm thick was obtained under these conditions. In order to avoid artifacts due to platinum deposition on fracture surfaces, preliminary experiments on the deposition of platinum on silicon single crystals were conducted under the same conditions. The size of platinum particles on single crystal faces was 4–5 nm in the given deposition regime.

The increase in the temperature of a sample during scanning, as estimated via the Castaing formula [27], did not exceed 10°C. Sample regions with dimensions from 5 × 4.5 mm to 50 × 45 μm were investigated at a magnification factor of 10^6.

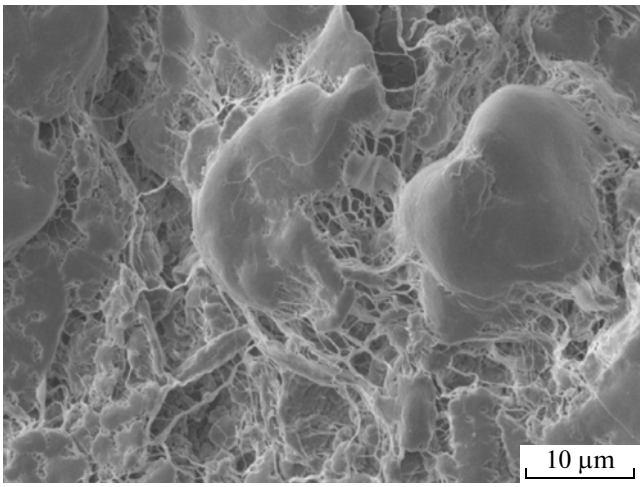

Fig. 1. A polymerizate particle of high-molecular-mass suspension-polymerized PTFE on the substrate.

RESULTS AND DISCUSSION

Morphology of Polymerizate Particles

It is well known that the primary product of PTFE polymerization is powder (polymerizate) particles with sizes from tens to several hundreds of microns. These are highly crystalline materials with a degree of crystallinity of 95–98%. Then, the powder is subjected to mechanical milling in order to attain the given dispersion parameters needed for subsequent molding and sintering.

To exclude the effect of mechanical impacts on the morphology of particles, polymerizate particles not subjected to milling were investigated. The sizes of the samples were in the range 0.1–1 mm.

As seen from Fig. 1, powder particles have an inhomogeneous structure. There are two types of domains: dense and fibrous. Fibrous domains form a continuum in which dense islet inclusions with a wide size distribution, from units to several tens of microns, are randomly dispersed.

Upon further magnification, it is found that single fibers possess a well distinguishable substructure (Fig. 2). They consist of several thinner fibrils, as indicated by the presence of deep longitudinal grooves and by the flat configuration of fibers. (The width is greater than the thickness.) Therefore, the fibers may be classified as ribbons consisting of fibrils. The fibrils are oriented along the direction of the ribbons. The least recognizable fibril diameter is ~15 nm.

Macromolecules are extended along the direction of fibrils (and ribbons) because the mean length of polymer chains is on the order of 10 μm for the studied polymer with $M \sim 10^7$, and the folding of chains within such a thin fiber (15–20 nm) seems improbable. The length of the fibrils reaches several tens of microns and

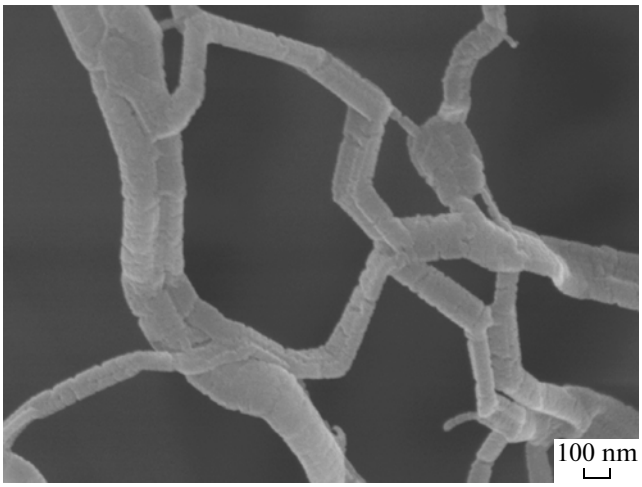

Fig. 2. Fibrous (filamentary) structures in the as-polymerized high-molecular-mass PTFE.

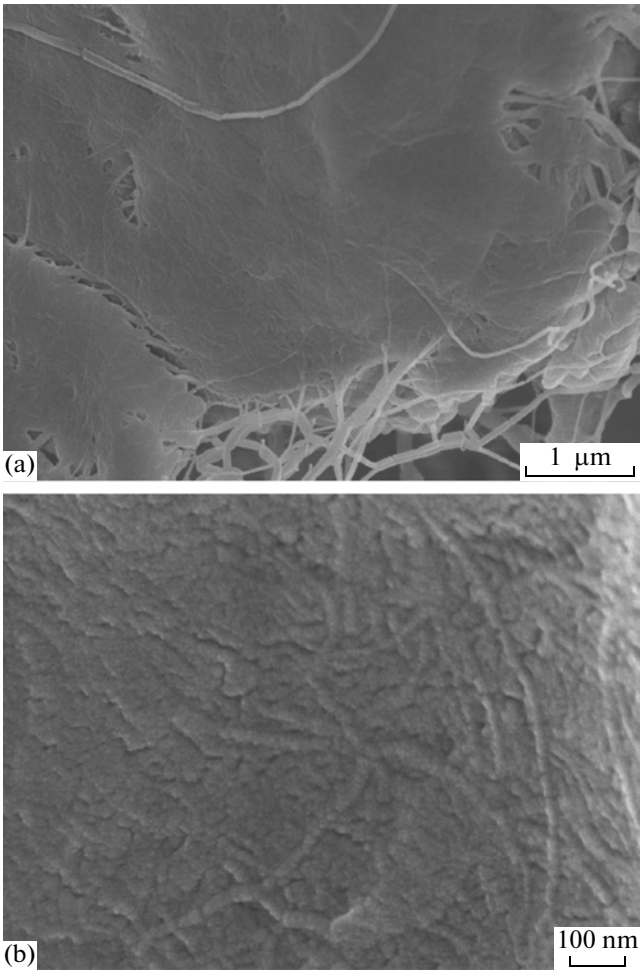

Fig. 3. Typical regions of dense domains of the PTFE polymerizate: (a) dense domains with discontinuities (pores) and (b) fibrillar structures in dense domains.

thus exceeds the macromolecular length. With allowance for the high (close to 100%) crystallinity of polymerizate particles, it may be concluded that the observed fibers are fibrillar crystallites formed by extended polymer chains.

Dense domains have apertures of discontinuity (pores) (Fig. 3a). A fibrillar structure is clearly seen on images of dense domains at a higher magnification (Fig. 3b). In general, the structure of these domains may be characterized as an assembly of densely packed fibrils. Underlying layers with an analogous fibrillar structure are seen deep in the pores (Fig. 3a).

Thus, the morphology of polymerizate particles is a combination of a network of ribbons, each of which may include several fibrils oriented along the ribbons, and blocks, consisting of densely packed fibrils. The conclusion about the fibrillar structure of the raw PTFE is in agreement with the experimental data [19, 20, 24], while the occurrence of a network structure correlates with the fact that the porosity of PTFE polymerizate particles is high [28].

Morphology of Sintered Samples

Further processing of the polymerizate via cold (at room temperature) molding and sintering yields PTFE articles in the form of blocks. However, the extremely high viscosity of PTFE ($\sim 10^{11}$ Pa s) is preserved at the sintering temperature (370–380°C) [29, 30]. Therefore, the sintering process aimed at coalescence (fusion) of powder particles is significantly hindered. This circumstance may lead to partial retention of porous dense domains and fibrillar ribbonlike structures inherent of polymerizate particles. This assumption is indirectly confirmed by the results of [23], where the sintering of powder particles caused no changes in the supramolecular structure. Furthermore, it may be assumed that the high viscosity of the PTFE melt facilitates preservation of the system of pores between powder particles after their sintering. The porosity of sintered PTFE was discussed in [31].

Let us consider SEM images obtained for fracture surfaces of sintered PTFE samples. We investigated two types of fracture surfaces: across and along the axis of sample molding. In what follows, they are referred to as TD (transverse direction) and MD (machine direction) fracture surfaces, respectively.

As is seen in Fig. 4, two regions, dense (homogeneous) and loose (porous), are formed on the surface of TD fracture surfaces. Dense regions have a fibrillar structure and are morphologically identical to those in polymerizate particles (Fig. 5). As regards these regions, it may be affirmed that sintering does not affect their structure.

In loose regions, as in polymerizate particles, there are single ribbons consisting of several fibrils oriented along a ribbon (Fig. 6). However, in contrast to the surface of raw PTFE, the fracture surfaces of sintered

samples have ordered structures in the form of bands with widths of 100–300 nm and lengths of several microns (Fig. 6a). As noted above, the band structure of the fracture surfaces of sintered PTFE has long been known [15], but their interpretation is ambiguous [15–17, 20, 23].

The use of high-resolution electron microscopy in the present study made it possible, in the authors' opinion, to convincingly demonstrate the fibrillar structure of the bands.

As is clear from Fig. 6, the bands consist of fibrils packed in parallel that are oriented across the direction of bands. Moreover, the bands are formed by passing fibrils whose ends go into the disordered polymer regions (Fig. 6b). Fibrils may participate in the formation of several ordered bands. A sharp boundary of a stripe is formed by the end regions of fibrils.

It appears that the fibrils are bound via amorphization of their surfaces during sintering. This phenomenon promotes partial interpenetration of fibrils (i.e., appearance of tie polymer chains involved in the formation of crystallites in two or more fibrils).

The morphologies of TD and MD fracture surfaces are different. A comparable amount of dense and loose domains is absent from MD fracture surfaces (Figs. 4, 7a). At low magnifications, the fracture surface seems to be homogeneous. Then, with a decrease in the scale, structures in the form of bands and single fibrillar ribbons, as well as pores, are predominantly found. Figures 7b and 7c obtained at high magnifications show that the packing density of fibrils and, accordingly, the thickness of amorphous interlayers between the fibrils vary within a single stripe.

It may be assumed that the fibrillar ribbons observed in polymerizate particles (Fig. 2) are capable of binding and forming ordered structures during processing (molding, sintering, and further crystallization). These structures are shaped as fibrillar lamellas extended perpendicularly to the orientation direction of fibril regions. The formation of band structure on the surface during sample fracture might be facilitated by the layer-by-layer structure of blocks, in which the bonding between fibrils within the layer is stronger than that between layers. In addition, an analysis of images makes it possible to conclude that the fibrils in lamellas have a less dense packing than dense domains in both the polymerizate and the sintered PTFE (Figs. 3b, 5, 6b, and 7b).

As follows from the above data, a fibril is an elementary unit for all observed morphological forms. The images presented in Figs. 6b and 7b) show that a fibril has a characteristic substructure. The fibril is a sequence of "beads" separated by a sharp electron contrast. The characteristic grain size of the substructure is 15–20 nm.

Thus, the main feature observed on the SEM images of fracture surfaces of sintered PTFE, in comparison with the SEM images of the surfaces polymerizate particles, is the formation of ordered fibrillar structures in the form of bands oriented perpendicularly to the direction of fibrils. Pores and single fibrillar ribbons typical for polymerizate particles are likewise observed on fracture surfaces of the sintered PTFE.

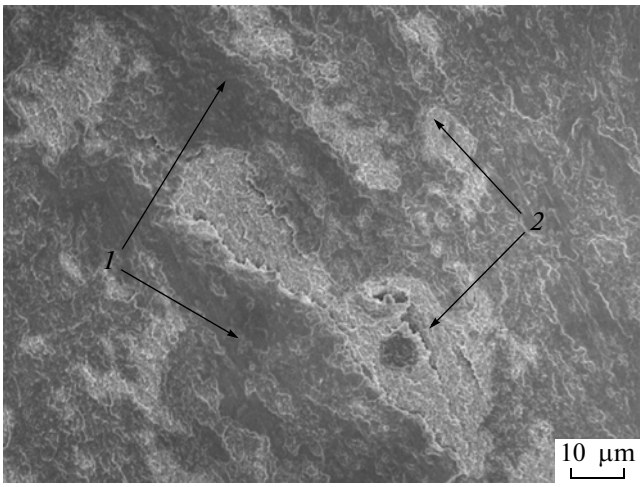

Fig. 4. (*1*) Dense and (*2*) loose domains of the TD fracture surfaces of the sintered PTFE.

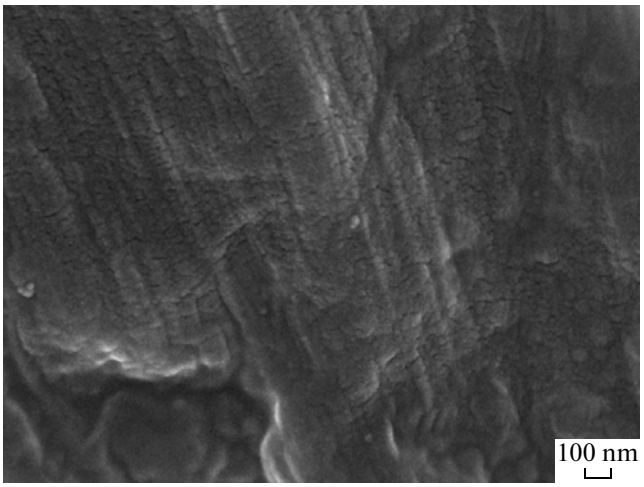

Fig. 5. Dense domains of the TD fracture surface of the sintered PTFE.

Morphology of Irradiated Modifications of PTFE

PTFE belongs to the type of polymers that undergo destruction under ionizing irradiation. The signs of destruction are the accumulation of end macroradicals formed via the scission of polymer chains, isolation of low-molecular-mass fluorocarbon radiolysis products, and a decrease in mechanical strength [32–34]. The radiation resistance expressed quantitatively via the dose of a half-decrease in the mechanical strength is abnormally low, by more than two orders of

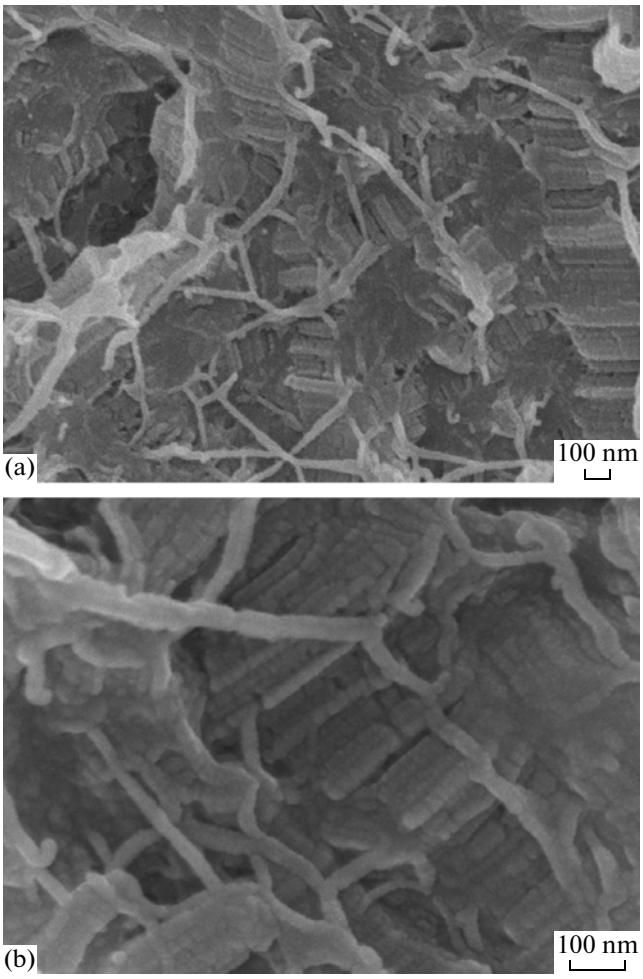

Fig. 6. Fibrillar structure of loose domains of the TD fracture surface of the sintered PTFE at magnifications of (a) 100000 and (b) 200000.

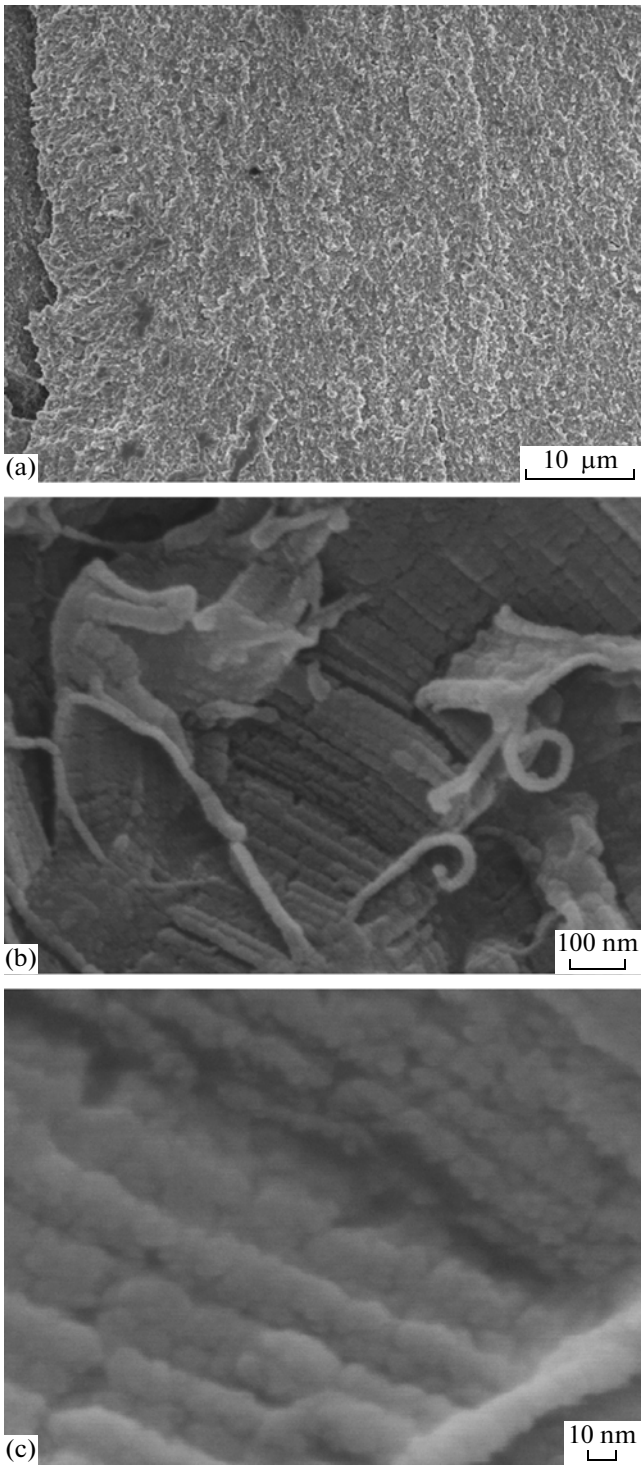

Fig. 7. Typical images of the MD fracture surface of sintered PTFE at magnifications of (a) 2000, (b) 100000, and (c) 500000.

magnitude relative to other polymers undergoing destruction (PMMA, PB, PETF, etc.). An increase in the radiation temperature is accompanied by a further increase in the yield of degradation and, correspondingly, by a decline in the radiation resistance [34].

However, above the melting point, the monotonic character of the temperature dependences of PTFE characteristics is violated. As was proposed in [1, 6], the irradiation of melted PTFE leads to a change in the direction of radiation-chemical processes, that is, to crosslinking and improvement of mechanical properties rather than destruction of polymer chains. Earlier, the features of the behavior of PTFE during its irradiation above the melting temperature were observed in [35], while crosslinking was assumed in [36–38].

In addition, in [10, 36], a change in the polymer morphology due to accumulation of the products of radiation destruction (chain scission, short-chain branches, isolated double bonds, low-molecular-mass products, etc.) was discussed as a possible cause of the abnormal behavior of PTFE near the melting temperature.

Below, the data of the comparative investigation of the morphology of sintered PTFE irradiated below

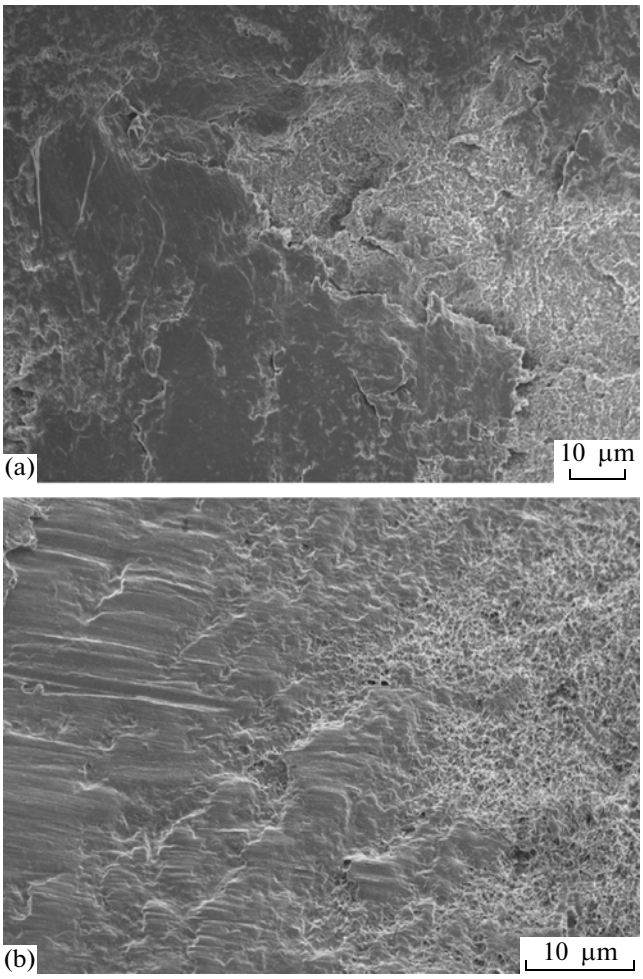

Fig. 8. General appearance of the TD fracture surface of the sintered PTFE exposed to a dose of 200 kGy at temperatures of (a) 20 and (b) 200°C.

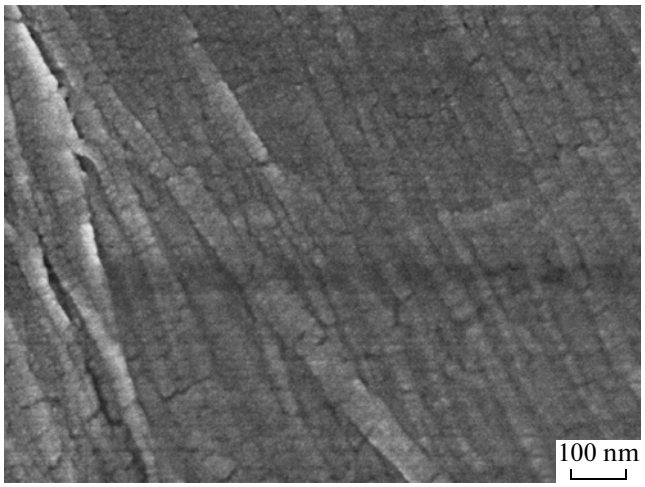

Fig. 9. Dense domain of the TD fracture surface of sintered PTFE exposed to a dose of 200 kGy at a temperature of 20°C.

and above the melting temperature of the crystalline phase are presented.

The morphologies of irradiated modifications of PTFE obtained at 20 and 200°C show some features common with the original nonirradiated polymer. In both cases, as for the original PTFE, dense and loose (porous) domains are observed on the fracture surfaces (Fig. 8). These domains consist of irregularly shaped blocks of densely packed fibrils (Fig. 9), single ribbons, and fibrillar lamellas (Fig. 10). An examination of the images makes it possible to conclude that all of the above speculations about the supramolecular structure and morphology of sintered PTFE are still valid for the irradiated PTFE.

An important feature observed for PTFE after its irradiation at 200°C is a noticeable broadening of bands (Fig. 10b).

On the basis of the concept of the lamellar-crystal nature of striated [20], it is difficult to explain their broadening during the irradiation of PTFE far below its melting temperature. An increase in the thickness of crystalline lamellas is usually observed during annealing in the region between the temperatures of melting and crystallization [39].

This fact may be explained under the assumption of the fibrillar structure of striated bands. It is known [32, 33] that the radiation-induced destruction (scission) of polymer chains occurs mainly in the amorphous phase, which possesses an increased free volume. The binding between fibrils is determined also by amorphous interlayers. Then, the destruction of macromolecules in the amorphous phase should lead to the weakening of bonds between fibrils, and their unpacked regions acquire the capacity for additional ordering, i.e., for the broadening of bands (or thickening of the fibrillar lamella).

The discussed explanation of the thickening of crystalline lamella plates implies an almost complete disruption of folds of macromolecules entering the disordered region on the surface of the crystalline lamella.

A qualitative change in the morphology of sintered PTFE occurs during its irradiation above the melting temperature of the crystalline phase. Centrosymmetric structures, that is, spherulites, are observed even at a low magnification (Figs. 11a, 12a). The sizes of spherulites amount to tens of microns. Figure 11 presents a part of the surface in which the centers of spherulites have the appearance of bulges that appear as a result of fracture. A spherulite is divided into separate sectors (petals) by "spines" (defect regions radiating from the center) in the plane of the fracture surface image. As seen from Fig. 11b, spherulites are formed by radially oriented fibrils. The fibrils are densely packed near the center, while their packing density decreases with the distance from the center.

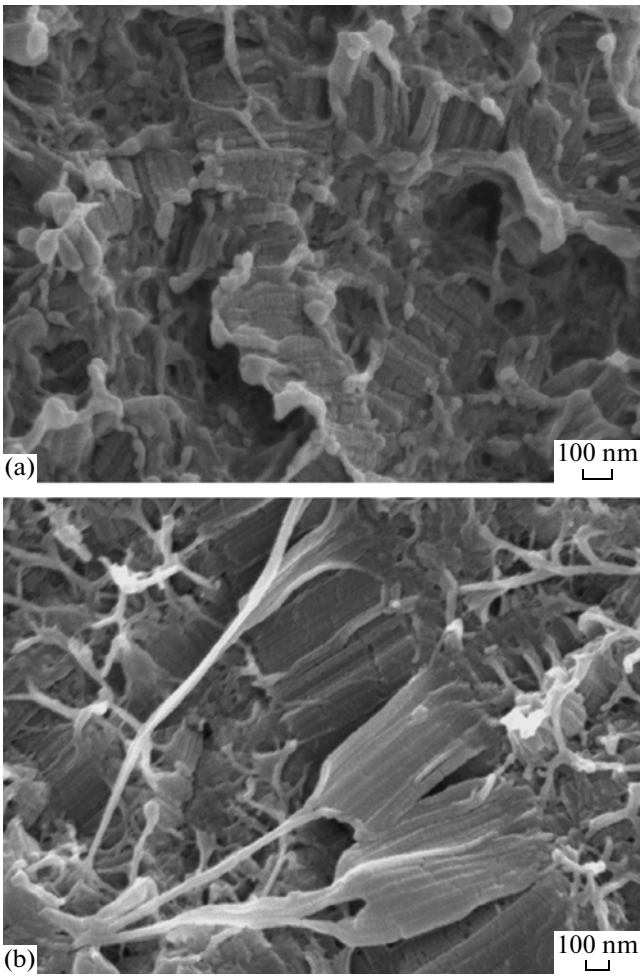

Fig. 10. Loose domain of the TD fracture surface of the sintered PTFE exposed to a dose of 200 kGy at temperatures of (a) 20 and (b) 200°C.

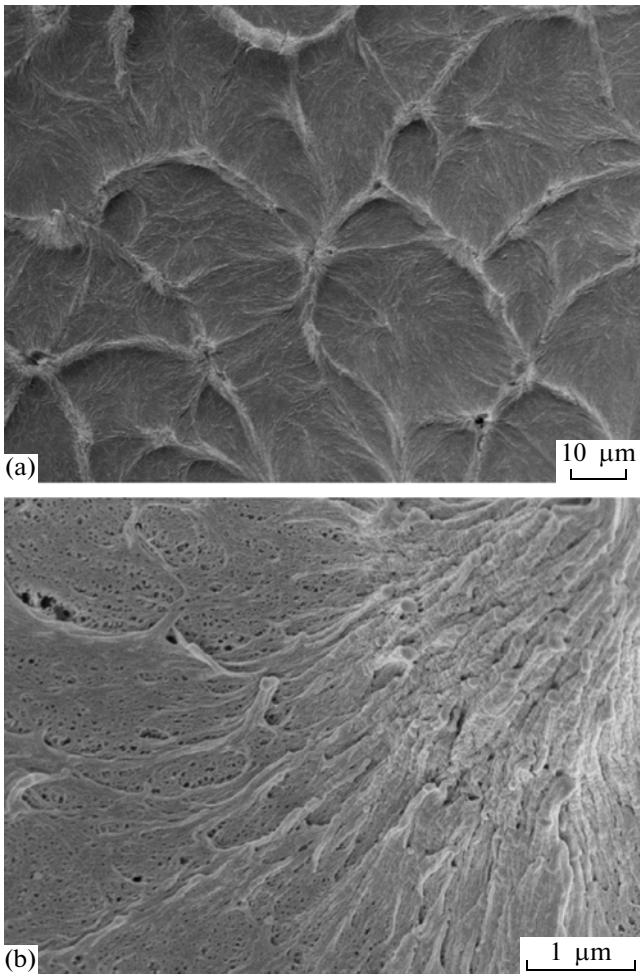

Fig. 11. TD fracture surface of PTFE exposed to a dose of 200 kGy at a temperature of 335°C. A part of the surface in which the centers of spherulites have the appearance of bulges that formed as a result of fracture: (a) spherulite structure and (b) fibrillar structure of spherulites.

Figure 12 shows regions with the response concave reliefs. Here, the centers of spherulite are craters and the boundaries of petals are concave. The peripheral interspherulite region is shown in Fig. 13. During the growth of spherulites, fibrillation of the structure leading to formation of a rare fibrillar network occurs owing to tensile stresses.

Thus, mutually responsive reliefs of spherulites are formed on two surfaces during fracture of the sample. Moreover, both convex and concave reliefs may be found on the same surface.

A comparative analysis of the images of fracture surfaces of PTFE irradiated below and above the melting temperature makes it possible to conclude that, on the whole, the spherulite structure of PTFE is less porous and lacks loose domains and pores with sizes from 100 nm or more. This assumption is consistent with a decrease in the porosity of PTFE irradiated in melt [29].

Earlier, the formation of spherulites was observed only for a low-molecular-mass emulsion polymerized PTFE ($M \sim 5 \times 10^5$) [18–20]. In [20], the spherulite structure was represented by radially oriented bands. In such spherulites, macromolecules are tangentially oriented because the bands are oriented perpendicularly to polymer chains. No spherulites were earlier observed in high-molecular-mass emulsion polymerized PTFE. However, as was shown above, this polymer almost fully transforms into the spherulite morphology during radiation modification above the melting temperature. In contrast to the low-molecular mass PTFE, fibrils and their constituent macromolecules are radially directed in the spherulites discovered in this study.

It is known that spherulites do form in high-molecular-mass PTFE. This circumstance is in agreement with the concept that the scission of macromolecular chains; the decrease in molecular mass; and, conse-

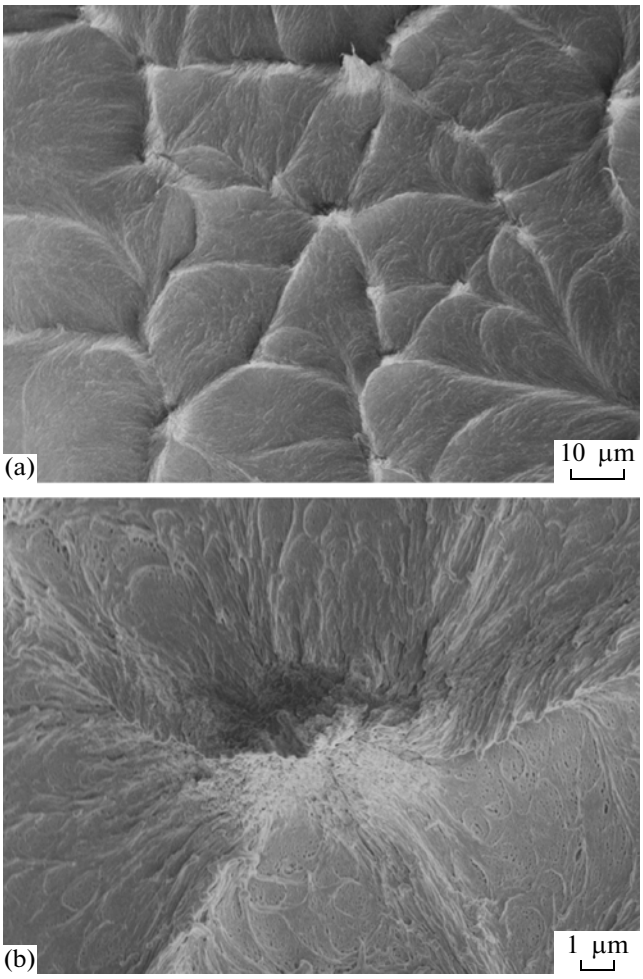

Fig. 12. TD fracture surface of PTFE exposed to a dose of 200 kGy at a temperature of 335°C. A part of the surface with the responsive concave relief, in which, as a result of fracture, (a) petals are concave and (b) centers of spherulites are craters.

quently, the reduction in melt viscosity comprise the main molecular mechanism of the radiation modification of high-molecular-mass PTFE in melt. The destruction of polymer chains decreases the binding between fibrils and increases their mobility. These factors promote the reorientation of fibrils with concomitant formation of spherulites that appear to be a morphological form preferable to fibrillar lamellas.

Thus, the specific feature of fibrils is their ability to generate different morphological forms: irregular densely packed blocks (in the polymerizate and in the sintered PTFE), lamellas (in the sintered PTFE), and spherulites (in the melt irradiated PTFE).

In addition, a decrease in the viscosity of melt facilitates the collapse of pores and voids inside the material due to surface-tension forces [29]. This shrinkage of pores in the modified samples may provide the direction of the structural rearrangement process and ensure the appearance of spherulite centers (nuclei).

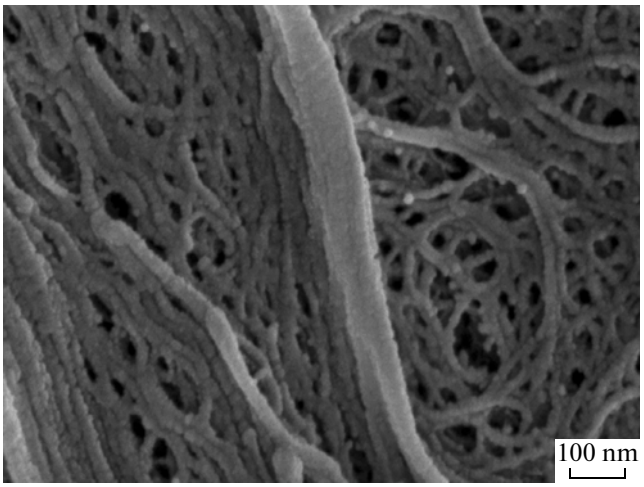

Fig. 13. Peripheral interspherulite region on the TD fracture surface of sintered PTFE exposed to a dose of 200 kGy at a temperature of 335°C.

A decrease in the porosity of PTFE, together with marked morphological changes, may result in a substantial enhancement of radiation-induced changes in macroscopic properties that are expected in the case when only molecular processes (destruction and/or crosslinking) occur.

CONCLUSIONS

The morphology of polymerizate particles of high-molecular-mass emulsion-polymerized PTFE is described as a combination of fibrillar ribbons that form a random three-dimensional porous network and blocks consisting of densely packed fibrils. The ribbons have a flat structure composed of several fibrils oriented along the ribbon direction.

The fibrillar supramolecular structure of the polymerizate is preserved after sintering. Morphological structures in the form of dense domains (blocks of densely packed fibrils) and single ribbons with the longitudinal orientation of fibrils are identical to those in the polymerizate. The distinctive feature of the sintered PTFE is that fibrillar lamellas extended perpendicularly to the direction of fibrils are formed.

The morphology of PTFE irradiated below the melting temperature at 20 and 200°C has some common features with the original nonirradiated polymer. In both cases, as well as for the original PTFE, dense and loose domains formed by fibrils are observed on the fracture surface. The specific feature found for PTFE after its irradiation at 200°C is a noticeable broadening of bands (the thickening of fibrillar lamellas).

Irradiation above the melting temperature leads to the complete structural reorganization of PTFE, that is, to the formation of new morphological forms—spherulites with sizes of several tens of microns that

consist of radially oriented fibrils—and, in general, to a considerable decrease in porosity. Such a structural reorganization of high-molecular-mass suspension-polymerized PTFE has been observed for the first time. It has been concluded that the formation of spherulites is caused by radiation-induced scission of polymer chains, a decrease in their molecular masses, and a reduction in polymer viscosity.

REFERENCES

1. J. Sun, Y. Zhang, and X. Zhong, Polymer **35**, 2881 (1994).
2. A. Oshima, K. Murata, T. Oka, N. Miyoshi, A. Matsuura, H. Kudo, T. Murakami, E. Katoh, M. Washio, and Y. Hama, Nucl. Instrum. Methods Phys. Res. B **265**, 314 (2007).
3. D. L. Pugmire, C. J. Wetteland, W. S. Duncan, R. E. Lakis, and D. S. Schwartz, Polym. Degrad. Stab. **94**, 1533 (2009).
4. K. Lunkwitz, U. Lappan, and U. Scheler, J. Fluorine Chem. **125**, 863 (2004).
5. J. Sun, Y. Zhang, X. Zhong, and X. Zhu, Radiat. Phys. Chem. **44**, 655 (1994).
6. A. Oshima, T. Tabata, H. Kudoh, and T. Seguchi, Radiat. Phys. Chem. **45**, 269 (1995).
7. A. Oshima, S. Ikeda, T. Seguchi, and Y. Tabata, Radiat. Phys. Chem. **49**, 279 (1997).
8. A. Setogawa, H. Nishi, Y. Yamamoto, H. Kusano, and T. Asai, Hitachi Cable Rev., No. 21, 83 (2002).
9. S. A. Khatipov and N. A. Artamonov, Ref. Zh. Khim. **52** (3), 89 (2008).
10. S. A. Khatipov, E. M. Konova, and N. A. Artamonov, Ref. Zh. Khim. **52** (5), 64 (2008).
11. A. Oshima, S. Ikeda, T. Seguchi, and Y. Tabata, Radiat. Phys. Chem. **49**, 581 (1997).
12. A. Oshima, T. Seguchi, and Y. Tabata, Radiat. Phys. Chem. **50**, 601 (1997).
13. U. Lappan, U. Geisler, and K. Lunkwitz, J. Appl. Polym. Sci. **74**, 1571 (1999).
14. U. Lappan, U. Geisler, and K. Lunkwitz, Radiat. Phys. Chem. **59**, 317 (2000).
15. C. W. Bunn, A. J. Cobbold, and R. P. Palmer, J. Polym. Sci. **28**, 365 (1958).
16. C. J. Speerschneider and C. H. Li, J. Appl. Phys. **33**, 1871 (1962).
17. C. J. Speerschneider and C. H. Li, J. Appl. Phys. **34**, 3004 (1963).
18. T. Davidson, R. N. Gounder, D. K. Weber, and S. M. Wecker, in *Fluoropolymers 2: Properties*, Ed. by G. Hougham, P. E. Cassidy, K. Johns, and T. Davidson, (Plenum, New York, 1999), p. 3.
19. P. H. Geil, J. Yang, R. A. Williams, K. L. Petersen, T.-C. Long, and P. Xu, Adv. Polym. Sci. **180**, 89 (2005).
20. L. Melillo and B. Wunderlich, Kolloid Z. Z. Polym. **250**, 417 (1972).
21. B. Wunderlich, *Macromolecular Physics, Vol. 1. Crystal Structure, Morphology, Defects* (Academic, New York, 1973; Mir, Moscow, 1976).
22. R. Androsch, B. Wunderlich, and H.-J. Radusch, J. Therm. Anal. Calorim. **79**, 615 (2005).
23. S. V. Kostromina, Yu. A. Zubov, N. G. Shirina, and Yu. Ya. Tomashpol'skii, Vysokomol. Soedin., Ser. A **32**, 445 (1990).
24. G. Butenuth, Verh.- Kolloid-Ges. **18**, 168 (1958).
25. T. Suwa, M. Takeshita, and S. Machi, J. Appl. Polym. Sci. **17**, 3253 (1973).
26. S. A. Khatipov, D. I. Seliverstov, and V. P. Sichkar', RF Patent No. 82 589 (2009).
27. R. Castaing and A. Guinner, Adv. Electron. Phys. **13**, 317 (1960).
28. Yu. A. Panshin, S. G. Malkevich, and Ts. S. Dunaevskaya, *Fluoroplastics* (Khimiya, Leningrad, 1978) [in Russian].
29. L. G. Case, J. Appl. Polym. Sci. **3**, 254 (1960).
30. K. Matsumae, M. Watanabe, A. Nasuoka, and T. Ichimiya, J. Polym. Sci. **28**, 653 (1958).
31. S. A. Khatipov, C. P. Kabanov, E. M. Konova, and S. A. Ivanov, Polymer Science (in press).
32. *Radiation Chemistry of Macromolecules*, Ed. by M. Dole (Academic, New York, 1972; Mir, Moscow, 1983).
33. V. K. Milinchuk, E. R. Klinshpont, and S. Ya. Pshezhetskii, *Macroradicals* (Khimiya, Moscow, 1980) [in Russian].
34. *Fluoropolymers*, Ed. by L. A. Wall (Wiley, New York, 1972; Mir, Moscow, 1975).
35. L. P. Yanova and A. B. Taubman, in *Effects of Ionizing Radiation on Inorganic and Organic Systems*, Ed. by S. Ya. Pshezhetskii (Akad. Nauk SSSR, Moscow, 1958), p. 314.
36. M. Tutiya, Jpn. J. Appl. Phys. **11**, 1542 (1972).
37. I. M. Abramova, L. G. Kazaryan, and V. S. Tikhomirov, Vysokomol. Soedin., Ser. B **17**, 572 (1975).
38. I. M. Abramova, L. G. Kazaryan, N. I. Bol'shakova, and V. S. Tikhomirov, Vysokomol. Soedin., Ser. B **32**, 28 (1991).
39. B. Wunderlich, *Macromolecular Physics. Vol. 2. Crystal Nucleation, Growth and Annealing* (Academic, New York, 1976; Mir, Moscow, 1979).